Predictions and Observations of Global Beta-induced Alfvén-acoustic Modes in JET and NSTX *

N. N. Gorelenkov[♯◇], H. L. Berk[♮], N.A. Crocker[o], E. D. Fredrickson[♯], S. Kaye[♯], S. Kubota[o], H. Park[♯], W. Peebles[o], S. A. Sabbagh[‖], S. E. Sharapov[♭], D. Stutmat[△], K. Tritz[△], F. M. Levinton[√], H. Yuh[√] and the NSTX team and JET EFDA Contributors[†]

[♯]*Princeton Plasma Physics Laboratory, Princeton University, Princeton, New Jersey 08543*

[♮]*Institute for Fusion Studies, University of Texas, Austin, TX, 78712*

[o]*University of California, Los Angeles, California 90095-1354*

[‖]*Columbia University, New York, New York 10027-6902*

[♭]*Euroatom/UKAEA Fusion Association, Culham Science Centre, Abingdon, Oxfordshire OX14 3DB, United Kingdom*

[△]*Johns Hopkins University, Baltimore, Maryland 21218 and*

[√]*Nova Photonics, Princeton, New Jersey 08543*

Abstract

In this paper we report on observations and interpretations of a new class of global MHD eigenmode solutions arising in gaps in the low frequency Alfvén -acoustic continuum below the geodesic acoustic mode (GAM) frequency. These modes have been just reported [1] where preliminary comparisons indicate qualitative agreement between theory and experiment. Here we show more quantitative comparison emphasizing recent NSTX experiments on the observations of the global eigenmodes, referred to as Beta-induced Alfvén - Acoustic Eigenmodes (BAAE), which exist near the extrema of the Alfvén - acoustic continuum. In accordance to the linear dispersion relations, the frequency of these modes may shift as the safety factor, q, profile relaxes. We show that BAAEs can be responsible for observations in JET plasmas at relatively low beta $< 2\%$ as well as in NSTX plasmas at relatively high beta $> 20\%$. In NSTX plasma observed magnetic activity has the same properties as predicted by theory for the mode structure and the frequency. Found numerically in NOVA simulations BAAEs are used to explain observed properties of relatively low frequency experimental signals seen in NSTX and JET tokamaks.

*This work supported in part by the U.S. Department of Energy under the contracts DE-AC02-76CH03073 and DE-FG03-96ER-54346 and in part by the European Fusion Development Agreement

†See Appendix of M. L. Watkins *et.al.,* Fusion Energy 2006 (Proc. 21$^{\rm st}$ Int. Conf. Chengdu, 2006) IAEA, Vienna (2006)

◇Electronic address: ngorelen@pppl.gov

I. INTRODUCTION

Recently the existence of Beta-induced Alfvén - Acoustic Eigenmodes (BAAE) was predicted [1, 2] theoretically. Initial comparisons with JET and NSTX experimental observations support identification of the low frequency magnetic activity as BAAE excitations. The shear Alfvén branch is relatively well studied especially in connection with the Toroidicity - induced and Reversed Shear Alfvén Eigenmodes [TAE and RSAE, also known as Alfvén Cascades], whereas modes depending on the interaction of the fundamental Alfvén and acoustic excitations, is less studied both theoretically and experimentally [3–6]. This interaction is mediated by finite pressure, plasma compressibility and the geodesic curvature. As a result additional gaps in the coupled Alfvén - acoustic continuum emerge [6, 7].

Recently a theoretical description of the ideal MHD Alfvén - acoustic continuum gap in the limit of low beta and high aspect ratio plasma [1] was studied. Earlier theoretical work of [6] was replicated. In addition, numerical studies found new global eigenmodes, BAAEs, and they arise near the extrema points of the continuum in both low and high beta plasmas. Experimental observations, generally qualitatively (in some cases quantitatively) support the numerical predictions of the mode frequency. Specifically, ideal MHD simulated BAAE frequency evolution qualitatively agrees with JET observations at low plasma beta 2%, although the predicted frequency is higher by a factor of 1.77 at the maximum frequency at which these modes are observed. The lowest value for the frequency that ideal MHD can predict is when there is negligible ion pressure and hot thermal electrons pressure with a unity adiabatic index. There still remains the challenge of matching all the numerical predictions with the experimental results. The principal difficulty is that the predicted frequency is more than the expected experimental observations. Perharps more accurate measurements of the q-profile can resolve the difficulty.

In NSTX with plasma the beta around 20% the expected frequency seems to be matched to the experimentally observed data, although strong toroidal rotation makes the precise frequency comparison difficult. BAAE mode structure and the polarization data agree with the theoretical predictions within the numerical uncertainty during the flattop phase of the analyzed plasma.

In Ref.[1] it was argued that particular value of specific heat ratio γ that was used as well as kinetic effects such as due to thermal ion FLR and non-perturbative interaction with

energetic particles may be responsible for the mismatch in computed and measured mode frequencies in JET. Another potential way to reconcile simulations and observation in JET is to assume that q-profile was different from the one used in simulations. For example, the use of slightly reversed q-profile or higher q_0 value would be favorable for the theory-experiment comparison. In this paper we elaborate more along the lines of these arguments theoretically. Experimentally we present the data from the dedicated NSTX experiments, where the safety factor profile was measured with the MSE diagnostic and where good theory-experiment agreement for the mode structure, frequency (and their evolution) was observed.

The analysis of the paper is within the ideal MHD theory, which is valid if the kinetic effects can be neglected such as in the case of low thermal ion temperature. Neutron measurements from JET show much weaker neutron signal at the beginning of the discharge (when BAAEs are observed), than at a later time during the discharge when $T_i \simeq T_e$ was measured. This indicates that at the time of BAAE observations assumption of $T_i < T_e$ can be made and the kinetic effects due to ion FLR can be neglected. However, in NSTX plasma measurements show that $T_i \simeq T_e$ and for the proper treatment of the problem one has to evaluate the kinetic effect. We will consider such effects in future publications and will focus in this paper on how well ideal MHD can describe low frequency observations in JET and in NSTX.

We note, that by understanding the range of BAAE frequency excitation and observing or exciting these frequencies in experiments we may be able potentially to extend the use of MHD to determine q_0 (and/or q_{min}). Such observations could be a very important diagnostic tool for ITER and other burning plasma experiments. This observation would also help to infer the central plasma beta and the ion and electron temperatures.

The paper is organized as follows. In section II we outline the derivation of the Alfvén - acoustic continuum and its extremum points and the frequency gap. We apply theory and NOVA simulations to JET and NSTX plasmas in Sections III and IV, respectively. Summary is given in Sec. V.

II. LOW FREQUENCY ALFVÉN - ACOUSTIC CONTINUUM

We start from the ideal MHD equations for the continuum, which incorporates both the shear Alfvén and the acoustic branches (neglecting drift effects) [8, 9]

$$\begin{aligned} \omega^2\rho\frac{|\nabla\psi|^2}{B^2}\xi_s + (\mathbf{B}\cdot\nabla)\frac{|\nabla\psi|^2}{B^2}(\mathbf{B}\cdot\nabla)\xi_s \; &+\gamma p k_s \nabla\cdot\vec{\xi} = 0, \\ \left(\frac{\gamma p}{B^2}+1\right)\nabla\cdot\vec{\xi} + \frac{\gamma p}{\omega^2\rho}(\mathbf{B}\cdot\nabla)\frac{\mathbf{B}\cdot\nabla}{B^2}\nabla\cdot\vec{\xi} \quad &+k_s\xi_s \quad = 0, \end{aligned} \tag{1}$$

where ψ is the poloidal magnetic flux, p and ρ are the plasma equilibrium pressure and density, γ is the specific heat ratio, $\xi_s \equiv \vec{\xi}\cdot[\mathbf{B}\times\nabla\psi]/|\nabla\psi|^2$, $\vec{\xi}$ is the plasma displacement, $k_s \equiv 2\mathbf{k}\cdot[\mathbf{B}\times\nabla\psi]/|\nabla\psi|^2$ and $\mathbf{k}$ and $\mathbf{B}$ are vectors of the magnetic curvature and field. The baseline physics of the Alfvén - acoustic mode coupling and the formation of the continuum and global modes in toroidal geometry can be understood in the limit of a low beta, high aspect ratio plasma. Making use of this tokamak ordering we find that the expression for the geodesic curvature is, $k_s = 2\varepsilon\sin\theta/q$, where $\varepsilon = r/R \ll 1$ and we neglected corrections of order $O(\varepsilon^2)$ and higher. This is justified for the low mode frequency, such that $\Omega^2 = O(1)$, where we defined $\Omega^2 \equiv (\omega R_0/v_A)^2/\delta$ and $\delta \equiv \gamma\beta/2 = O(\varepsilon^2)$. Thus, keeping only leading order terms we reduce the system of equations Eq.(1) to (for details see Ref.[10])

$$\Omega^2 y + \delta^{-1}\partial_\parallel^2 y \quad +2\sin\theta\, z \quad = 0, \tag{2}$$

$$\Omega^2 z + \partial_\parallel^2 z \; +2\Omega^2\sin\theta\, y \; = 0, \tag{3}$$

where $y \equiv \xi_s\varepsilon/q$, $z \equiv \nabla\cdot\vec{\xi}$, $\partial_\parallel \equiv R_0 d/dl$ and l is the distance along the field line. For sufficiently small values of ε and β, numerical solutions of Eqs.(1,3) are found to be almost identical to numerical solutions of the NOVA code [8], which solves Eqs.(1). For this section, we can then consider Eqs.(1) and (2,3) to be interchangeable.

Equation (2) is essentially the shear Alfvén wave equation if z term is neglected. Equation (3) for z alone, would be the conventional sound equation. The two equations couple due to the finite compressibility of the plasma in toroidal geometry to give the form shown in Eqs.(2, 3). The coupling of each branch with the dominant poloidal mode number m, is via the $m\pm1$ sideband harmonics of the other branch. To treat the side band harmonics we employ the following form for the perturbed quantities

$$\begin{pmatrix} y \\ z \end{pmatrix} = \sum_j \begin{pmatrix} y_{j-m}(r) \\ z_{j-m}(r) \end{pmatrix} e^{-i\omega t + ij\theta - in\zeta}, \tag{4}$$

where ζ is the ignorable toroidal angle along the torus, the direction of symmetry.

By substituting Eq.(4) into Eqs.(2,3) to eliminate $z_{j\pm1}$ in terms of y_j and $y_{j\pm2}$ we find a three term recursion relation

$$\left[\Omega^2 - \frac{k_j^2}{\delta} - \Omega^2\left(\frac{1}{\Omega^2 - k_{j-1}^2} + \frac{1}{\Omega^2 - k_{j+1}^2}\right)\right] y_j + \Omega^2\left[\frac{y_{j-2}}{\Omega^2 - k_{j-1}^2} + \frac{y_{j+2}}{\Omega^2 - k_{j+1}^2}\right] = 0.$$

One can readily justify that for $j = 0$ we can ignore the side band terms in the limit $\delta \ll 1$. Then the coefficient of y_0 must vanish and we obtain the following dispersion relation (similar to Ref.[6])

$$\left(\Omega^2 - k_0^2/\delta\right)\left(\Omega^2 - k_{+1}^2\right)\left(\Omega^2 - k_{-1}^2\right) \;=\; \Omega^2\left(2\Omega^2 - k_{+1}^2 - k_{-1}^2\right). \tag{5}$$

The left hand side set to zero, represents oscillations in an infinite medium, the two acoustic modes $\Omega^2 = k_{\pm1}^2$ and the shear Alfvén wave $\Omega^2 = k_0^2/\delta$, in the absence of toroidal effects and this is valid for $k_0^2/\delta \gg 1$. However the character of the solutions drastically changes for $k_0^2/\delta \ll 1$.

Then as $|k_{\pm1}| \gg |k_0|$ in the vicinity of $q = m/n$ we can approximate $k_j^2 = (j/q + k_0)^2 \simeq j^2/q^2 + 2k_0 j/q$. Note, that in the high- m, n limit the radial dependence can be kept in the k_0 term only and $q = q_r = m/n$ can be fixed at the rational surface value, that is $k_j^2 \simeq j^2/q_r^2 + 2k_0 j/q_r$. With the coupling effect from the geodesic curvature, we find in the limit $k_0^2/\delta \ll 1$ two low frequency roots. One is

$$\Omega^2 = 1/q^2 \tag{6}$$

(comparable in frequency to the two acoustic side band frequencies), while the second solution takes the form of a modified shear Alfvén wave

$$\Omega^2 = k_0^2/\delta\left(1 + 2q^2\right). \tag{7}$$

This dispersion also follows from the kinetic theory developed in Ref.[11]. As k_0^2/δ gets larger the modified Alfvén wave frequency, Eq.(7), approaches the frequency of the first solution, Eq.(6), but do not cross. The first solution's frequency, Eq.(6), increases slowly, while the character of the Alfvénic branch solution, Eq.(7), changes dramatically and begins to decrease. As one increases k_0^2/δ further, so that it becomes larger than unity, the larger of the two roots approaches the acoustic side band solution

$$\Omega^2 = k_{\pm1}^2, \tag{8}$$

taken with plus sign (assuming $k_0 \gg \sqrt{\delta}$ or minus sign if $-k_0 \gg \sqrt{\delta}$) while the smaller of the two solutions (i.e. the modified Alfvén wave, Eq.(7) approaches the other acoustic sideband, Eq.(8), with minus sign (or plus sign if $-k_0 \gg \sqrt{\delta}$). The third root of the dispersion relation given by Eq.(5) in the limit $k_0^2/\delta \ll 1$ is found to be the geodesic acoustic mode (GAM) with a frequency which is larger than the other two modes, i.e. $\Omega^2 = 2\left(1 + 1/2q^2\right)$ [12–14]. As k_0^2/δ increases, this mode changes character and becomes the usual shear Alfvén wave $\Omega^2 = k_0^2/\delta$ when $k_0^2/\delta \gg 1$. The same branch was found in Refs. [15] and [4], but was called BAE branch.

As we indicated, when $k_0^2/\delta \sim 1/q^2$ Alfvén and acoustic branches approach each other, but their corresponding roots do not cross. Instead, they form a gap (in frequency) structure that needs to be resolved. Now, we can rewrite Eq.(5) in the following form $4k_0^4/\delta q_r^2 - A^2 k_0^2/\delta + \Omega^2\left(A-2\right)A = 0$, where $A = \Omega^2 - q_r^{-2}$. We can solve this equation for $k_0^2\left(\Omega^2\right)$ dependence:

$$k_0^2 = \left[A^2 \pm \sqrt{A^4 - 16\delta\Omega^2 A\left(A-2\right)/q_r^2}\right] q_r^2/8. \tag{9}$$

This dispersion contains the branches discussed above. We can make use of the properties of Eq.(9) to find the expression for the continuum frequency gap at which $\partial k_0^2/\partial\Omega^2 \to \infty$, that is where k_0^2 has double root. It is easy to see that one of such cases is when $A = 0$, which is found to be a root that corresponds to the upper boundary of the gap, $\Omega = \Omega_+$, where

$$\Omega_+^2 = 1/q_r^2. \tag{10}$$

To find the lower boundary of the gap we consider Eq.(9) together with the double root condition, and find that a cubic equation for A needs to be satisfied: $A^3 - 16\delta\left(A + q_r^{-2}\right)\left(A-2\right)/q_r^2 = 0$ or

$$\hat{A}^3 - \left(\hat{A} + b\right)\left(\hat{A} - d\right) = 0, \tag{11}$$

where $\hat{A} = q_r^2 A/16\delta$, $b = 1/16\delta$, and $d = 2q_r^2/16\delta$. An exact solution of Eq.(11) can be obtained in general form, but it can be accurately approximated assuming $2q_r^2 > 1$. We find then $\hat{A} = C^{1/3} - d/3C$, where $C = d\sqrt{4d + 27b^2}/6\sqrt{3} - bd/2 > 0$, and the lower boundary gap frequency is expressed by

$$\frac{\Omega_-^2}{\Omega_+^2} = 1 + 16\delta\left(C^{1/3} - \frac{d}{3C^{1/3}}\right). \tag{12}$$

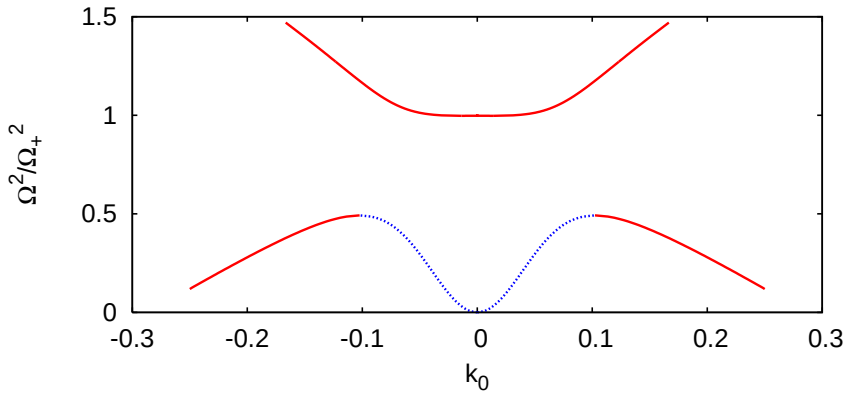

Figure 1: Solution of model dispersion relation as given by the Eq.(9), in high-m limit at $q = 1.75$. Plotted is the inverted dependence $k_0\left(\Omega^2\right)$. Solid, red line is acoustic branch of the continuum, whereas dashed blue line is the modified Alfvénic branch.

This can be further reduced in the limit of $\delta \ll 1$ to

$$\Omega_-^2 = \Omega_+^2\left[1 - \left(32q^2\delta\right)^{1/3}\right]. \tag{13}$$

However, this last form is accurate only for very low plasma beta, $\delta < 0.2\%$ (see Figure 2).

The graphical representation of the dispersion of the gap, Eq.(9), is shown in Figure 1 and depends only on k_0.

It follows from the analysis above and from Figure 1 that the gap width is on the order of the gap frequency. The frequency of two acoustic sideband branches is inside the gap as well as the frequency of the resonance between the Alfvén dominant harmonic mode and acoustic sideband, which is the lowest of two and can serve as a rough estimate for the center of the gap

$$k_0^2 = \frac{\delta\left(1+2q^2\right)}{q^2}\left(1+\sqrt{\delta\left(1+2q^2\right)}\right)^{-2},$$

and the center of the gap is at

$$\Omega_0 = \Omega_+ / \left(1+\sqrt{\delta\left(1+2q^2\right)}\right). \tag{14}$$

So that the approximate lower gap boundary is

$$\Omega_- = \Omega_0 - \Delta\Omega/2, \tag{15}$$

where $\Delta\Omega \simeq 2\Omega_+\sqrt{\delta\left(1+2q^2\right)} = 2\delta\sqrt{1+2q^2}/q$. We show different approximations for the BAAE gap boundaries in Figure 2.

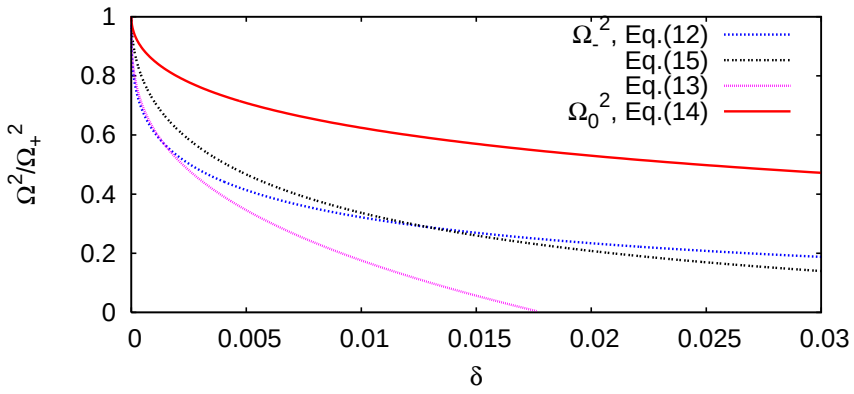

Figure 2: Comparison of the Alfvén/acoustic gap low boundary, Ω_-^2, following from different approximations (as indicated) of a an exact solution of Eq.(12) versus plasma beta parameter δ. Shown also is the frequency of the center of the gap, Ω_0^2. All frequencies are normalized to the upper boundary of the gap, Ω_+^2, given by Eq.(10).

The comparison of different continuum solutions obtained from Eqs.(2,3) and by NOVA code (from Eqs.(1)) for a specific case of circular surface plasma, based on the JET plasma, was done in Ref. [1]. It showed remarkable agreement, which validates the truncation procedure applied above.

III. SIMULATIONS AND OBSERVATIONS OF BAAES IN LOW BETA JET PLASMA

Measured spectrum of edge magnetic signal in JET, figure 3, shows low frequency signal evolution. One interesting and important observation is that only even mode numbers were observed $n = -2, 2, 4, 6$. The toroidal rotation has to be included in further quantitative analysis, but was not measured in the experiment. It can be evaluated by comparing different n's, for example $n = -2$ and 2 signals at $t = 6.6sec$, i.e. when they are equal frequencies in the lab frame. Assuming that both modes have the same radial location, one can infer the rotation frequency $f_{rot} \simeq 2kHz$. The same value for f_{rot} emerges by comparing $n = -2$, 2 and 4 mode frequencies at $t = 7.1sec$.

This discharge was numerically analyzed in Ref.[1] using NOVA code [8] under the assumption of monotonic q-profile. For each n number two modes were found, one in the center at low shear region and the other in the BAAE gap, near the top of the gap boundary. These

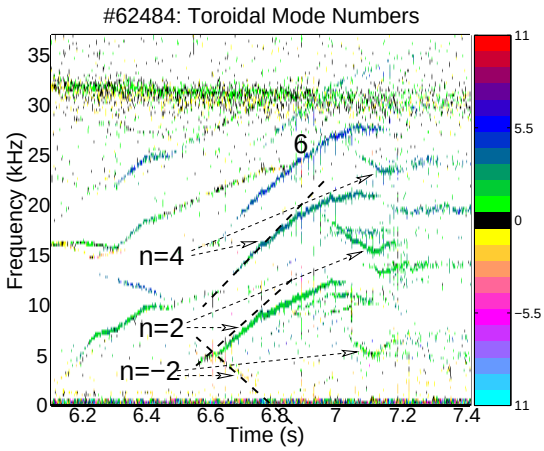

Figure 3: Magnetic signal frequency spectrum at the start of the discharge. Different colors represent different toroidal mode numbers corresponding to the color chart on the right. Black dashed lines are tangential to the signal initial evolution at $t = 6.6sec$.

are the locations where the continuum extrema points are formed (see also Fig.1). In the low shear region $\Omega(k_0)$ function is effectively stretched in radial direction, which also creates a local continuum extremum (similar to RSAE formation[16, 17]). However, the main problem previous JET simulations faced is the predicted BAAE frequency mismatch with the observations as we discussed in the introduction.

Here in order to show the sensitivity of the BAAE frequency to the safety factor profile we study weakly reversed shear plasma with otherwise the same plasma parameters as in Ref.[1]. The major radius is $R_0 = 2.90m$, the minor radius is $a = 0.95m$, the magnetic field is $B_0 = 2.7T$, the plasma beta profile is $\beta_{pl} = \beta_{pl0}\left[1 - (r/a)^2\right]^2$ %, $\beta_{pl0} = 1\%$, central electron density is $n_{e0} = 1.3 \times 10^{13} cm^{-3}$, safety factor profile is taken in the form described in Ref.[9] with edge value $q_1 = 4$, $q' = dq/d\Psi$ equal -0.2 and 30 at the center and at the edge respectively, so that q_{min} is at $r/a = 0.45$ (for example if $q_{min} = 0.99$ then at the center $q_0 = 1.012$), $r/a \equiv \sqrt{\Psi}$ and Ψ is the normalized poloidal flux, last closed magnetic surface ellipticity 1.7 and triangularity 0.23. Plasma pressure is assumed to have only electron contribution. Simulations suggest that to find global BAAEs we need to assume fairly extended region of low shear region near q_{min} surface. The plasma beta profile was fitted to measurements of the electron temperature and density, $T_{e0} = 6keV$. These plasma parameters correspond to the initial phase of JET discharge #62484, in which strong $\sim 2MW$ ICRH was applied.

We have found two global BAAEs, which are shown in figure 4 for $q_{min} = 0.99$. As q_{min} is

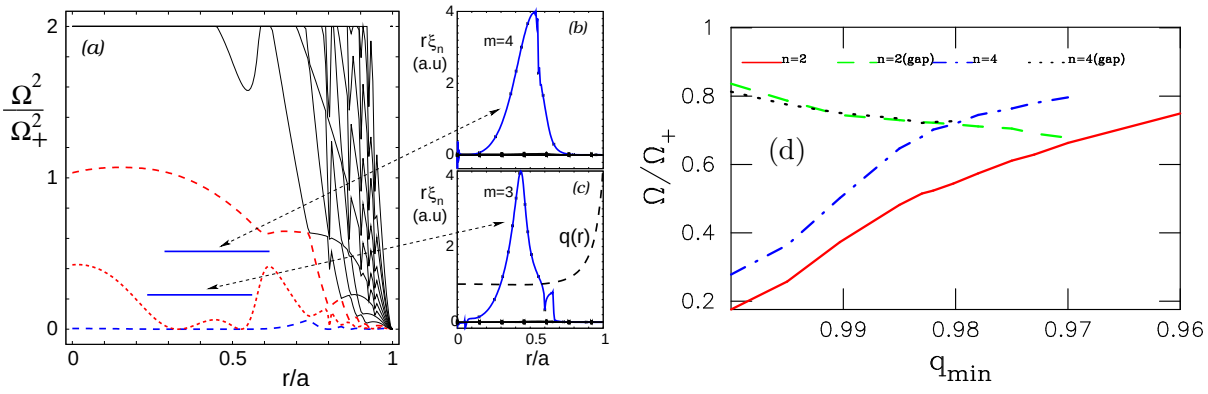

Figure 4: Alfvén - acoustic continuum (figure (a)) is shown as red dashed curves for JET reversed magnetic shear plasma for $n = 4$ and $q_{min} = 0.99$. The radial extent of two global BAAEs and their frequencies are shown as solid lines near the extremum points. The radial mode structure of BAAE located in the gap is shown in figure (b) as the structure of its dominant poloidal harmonic of the normal component of the plasma displacement vector in arbitrary units. Figure (c) shows the radial structure of core localized BAAE along with the weakly reversed q-profile. Figure (d) shows BAAE eigenfrequencies as functions of q_{min} for the slightly reversed q-profile with q_{min} at $r/a = 0.45$. Frequencies are normalized to Ω_+, which corresponds to $31kHz$. Shown in figure (d) are core localized mode frequencies for low shear $n = 2$ (solid red curve), $n = 2$ gap mode (dashed green curve), low shear $n = 4$ (blue dot-dashed curve) and gap mode $n = 4$ (short dashed black curve).

expected to decrease in time (due to plasma current diffusion) Alfvén - acoustic continuum evolves and so do the frequencies of BAAEs according to figure 4(d). The reversed shear plasma results are qualitatively similar to the results with the monotonic shear profile [1]. For example, the low shear localized mode frequency is limited by the lower gap frequency, Ω_-, and starts from a very small value. Numerically modes are not found near the lower extremum point inside the gap. This effect may be similar to the TAE frequency downshift effect due to the pressure gradient (eventually merging into the continuum near the gap)[10, 18]. Modes are robustly computed for both flat and slightly reversed q profiles.

The lowest value for BAAEa frequency is obtained if $\gamma = 1$, that is to use only electron beta for plasma equilibrium, $\beta_{pl0} = \beta_{e0} = 0.5\%$. This assumption seems to be consistent with the experimental conditions of strong H-minority heating and low plasma density, which means that ICRH power is primarily dumped into the electrons. Another indication of small

ion temperature is much weaker nuetron signal at the beginning of the discharge than at its flattop, at which point temperature were measured to be comparable. In the case of low ion temperature, we find that Ω_+ corresponds to $f = 31.7kHz$, which means that at the frequency crossing point of the low shear and gap BAAEs, $n = 4$ BAAE frequency is $0.7\Omega_+ \simeq 22kHz$. Again, like in Ref.[1] this value is above the measured frequency $f_{n=4} = 14kHz$ by 1.57 (compare with 1.77 factor for monotonic q-profile Ref.[1]).

A rather simple suggestion to resolve the frequency mismatch in JET is to assume the existence of local low (and reversed) shear region with $q_{min} = 1.5$. In that case $\Omega_+ \simeq 21kHz$, so that the monotonic q-profile would result in BAAE frequency $\sim 16kHz$, which is sufficiently close to observations. This conjecture would also solve the problem of observations of only even toroidal mode numbers, since $m = q_{min}n$ must be integer. We have to note, that at $t = 7sec$ sawteeth-like events have been seen by soft x-ray measurements of electron temperature. There are indications that $q_0 \simeq 1$. This still can be consistent with the existence of local $q_{min} = 1.5$ at some radii away from the plasma center. More experiments are required in order to validate theoretical predictions for BAAE frequency.

Finally, a potential reason behind the frequency mismatch is the model for γ, which so far was not properly tested in experiments and a more accurate kinetic treatment is needed. One kinetic effect arising from the ion drift frequency turns out to be negligible. For example for $n = 4$ we find that the drift frequency calculated with the pressure gradient is $\omega_{*pi}/\omega_+ = 1.7 \times 10^{-2}$. Hence, instabilities studied in Refs.[11, 15] can not explain the JET observations discussed in this paper. Finally, energetic particles, which seem to be exciting the BAAE instabilities may cause the shift between the computed and measured mode frequencies [19].

IV. OBSERVATIONS OF BAAES IN HIGH BETA NSTX PLASMA

Our theory predicts that at high plasma beta Alfvén and acoustic modes will be strongly coupled as δ becomes finite. Thus, it is important to explore high-β plasmas which are typical for spherical tokamaks. In addition the safety factor profile measurements with Motion Stark Effect (MSE) diagnostic in NSTX make such study very important for the quantitative validation of the theoretical predictions. A special experiment has been designed to verify the theory predictions and to attempt to reconcile theory-experiment discrepancy

obtained in JET analysis presented in previous section and in Ref.[1].

Similar conditions to the NSTX shot #115731 (described in Ref.[1]) were reproduced with more internal diagnostics applied for the purpose of mode identification. The following plasma parameters were achieved (at $t = 0.26s$ of the discharge) $R_0 = 0.855m$, $a = 0.66m$, safety factor as in figure 8(a), $\beta_{pl0} \equiv 2\pi p\left(0\right)/B_0^2 = 0.34$, vacuum magnetic field at the geometrical center $B_0 = 0.44T$, edge safety factor $q_1 \simeq 13.86$, $q_0 \simeq 2.1$, and the same $\gamma = 1.375$, which is consistent with the TRANSP modeling, i.e. $T_i \simeq T_e$, and follows from a kinetic theory [20].

NSTX magnetic activity spectrum evolution is shown in Figure 5. This figure shows typical NSTX magnetic activity at the beginning of the discharge. First, RSAEs are observed with sweeping frequencies up and down, which however has overall upward trend as the plasma beta is accumulated and thus TAE/RSAE frequencies are upshifted by the expanding BAE gap, the effect discussed theoretically in Refs.[4, 10, 13, 18, 21] and recently experimentally in Ref.[22]. After total beta reaches value of approximately 20% RSAE/TAE activity is suppressed, likely due expected mode frequency move into the continuum at high pressure gradients. Instead a lower frequency activity is often observed, such as marked BAAEs.

Figure 5 shows $n = 2, 4$ activity with frequencies from the level of plasma rotation ($f_{rot} \simeq 15kHz$) at q_{min} surface to about $50kHz$ (for $n = 2$ mode) in the lab frame. One can notice that at $t = 2.75s$ some kind of internal reconnection event happens, which brings BAAE frequency back to the level of plasma rotation (zero frequency in the plasma frame). This may indicate that q_{min} value is changed back to its value at $t = 2.62s$. Another interesting observation is that like in JET plasma only even n-number BAAEs have been observed at $t = 0.262 - 0.275s$.

MSE diagnostic measured q profile, results of which are shown in Figure 6 in the form of q_{min} evolution. We compare q_{min} MSE results with values inferred from RSAE and BAAE observations (see figure 5). Times when the spectrum of $n = 1$ RSAE magnetic activity approaches the envelop of upper BAE gap (GAM frequency, shown as dashed curve in Figure 5) serve as an indication of rational value of q_{min}. Such points are denoted as RSAE points in Figure 6. As it follows from our theory, BAAEs with minimum frequency are expected to be observed at rational values of q_{min}. From MSE and BAAE observations we infer that $q_{min} = 3/2$ at $t = 0.262s$. Note, that this value is also consistent with the even

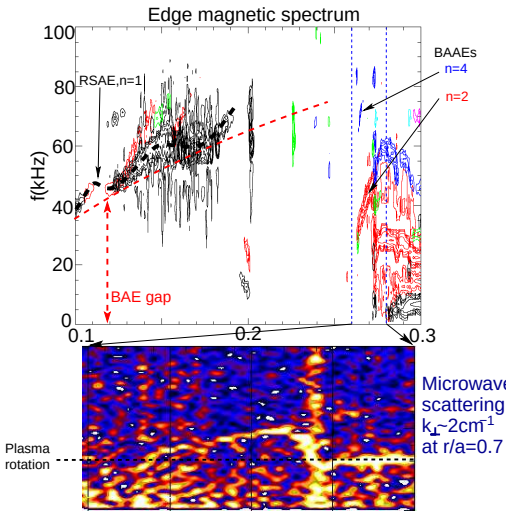

Figure 5: Magnetic activity spectrum evolution in NSTX discharge #123816 dedicated to BAAE study and shown from $t = 0.1 - 0.3s$ time range. Various identified activities are indicated such as $n = 1$ RSAE and $n = 2, 4$ BAAEs. Lower color figure corresponds to blown up time period of BAAE activity (vertical axis is the same) and is measured by the high-k scattering system, which diagnose the plasma displacement with a specific range up to radial wavevectors $k_r \simeq 12cm^{-1}$ at $R \simeq 1.45m$ (or $r/a \simeq 0.7$).

n-numbers observations, that is $m = q_{min}n$ must be integer.

We perform NOVA numerical analysis for the plasma of interest by scanning q_{min}. MHD continuum for $q_{min} = 1.43$ and $n = 2$ is shown in Figure 7(a), which also shows the radial extend and the frequency of the low shear global BAAE. Due to typically large beta of the plasma in NSTX BAAE gap becomes large and merges with otherwise wider BAE gap (we indicate them as one BAE/BAAE gap). However, like in JET, plasma continuum branches frequencies are still close to their cylindrical dispersion relations, indicated as A- and a-curves in 7(a). The global low-shear BAAE eigenfrequency follows closely the modified Alfvén continuum.

Numerically, we have found several global BAAEs for each q_{min} value in the scan. Shown in 7(b) are the BAAE eigenfrequency dependences for two plasma betas, $\beta_{pl0} = 18.5\%$ and $\beta_{pl0} = 34\%$. Shown frequencies correspond to either solutions closest in frequency to the continuum (low shear mode) with no radial nodes for $q_{min} = 1.5 - 1.35$, or to the gap modes for $q_{min} = 1.35 - 0.85$. Note, that such transition from low shear to the gap mode is

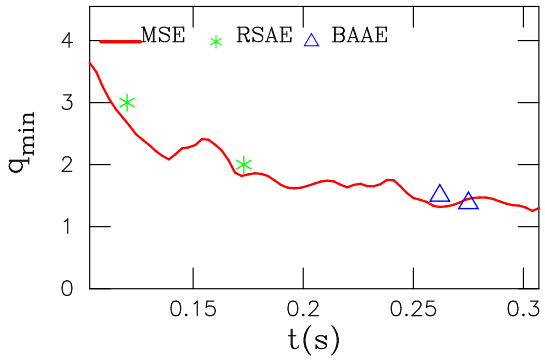

Figure 6: MSE measured evolution of q_{min} in the times of interest. Shown also are results of the comparison of the MHD RSAE and BAAE activities with the theoretical expectations for q_{min} values.

continuous in NSTX, whereas in JET the low shear sweeping frequency solution is separated in frequency from the gap solution as q decreases. This seems to be due to higher beta in NSTX. As one can see the absolute value of BAAE frequency at maximum of its frequency sweep in observations, i.e. $20kHz$ (corrected for the Doppler shift from $50kHz$ in the lab frame at $q_{min} = 1.38$, $t = 2.74$), does not reach the value of the gap BAAE frequency. We show this point as second BAAE point in Figure 6, which seems to predict q_{min} in reasonable agreement with MSE measurements.

Since BAAE is bounded radially by mth poloidal harmonic continuum we expected it to be radially strongly localized near q_{min} radius when BAAE frequency is at the bottom (near zero) of its sweep, that is when q_{min} is close to the rational value. As q_{min} decreases BAAE should broaden radially. Eventually, after entering the BAAE gap the mode structure is expected to be wide. This is similar to RSAE to TAE transition observed in DIII-D [23]. NOVA simulations support this as shown in Figures 8(a-c), where radial dependencies of the poloidal harmonics of BAAE plasma displacement normal to the surface component (in the form $r\xi_n(r)$) are presented. Figure 8(b) corresponds to $q_{min} = 1.376$, which is the second BAAE point in Figure 6, $t = 2.74s$. At that point BAAE is bounded by the continuum on the right, i.e. at $R = 1.35m$, so that the mode structure seems to be broadened toward the center.

We compare these theory predictions with the internal fluctuation structure measured by the Ultra-Soft X-Ray (USXR) fast camera diagnostic installed on NSTX. USXR diagnostic

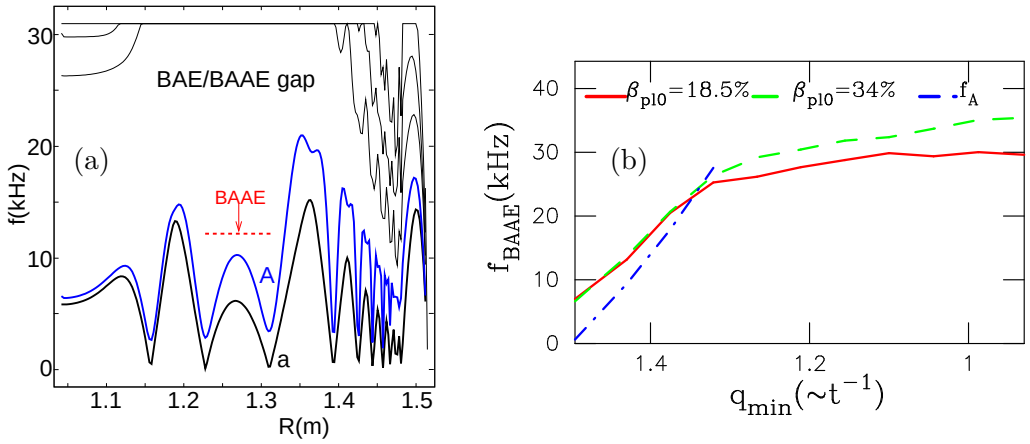

Figure 7: Shown in figure (a) are numerically simulated Alfvén - acoustic continuum and the position of BAAE (dashed horizontal line) for $n = 2$ and $q_{min} = 1.43$. Indicated are acoustic part (curve a) and the Alfvén part (curve A) of the continuum. Shown in figure (b) are frequencies of global BAAE modes as their frequencies sweep up versus q_{min} (approximately inversely proportional to time). We show BAAE eigenfrequency evolution for two plasma betas as indicated. Also shown is the expected modified Alfvénic branch continuum frequency, Eq.(7).

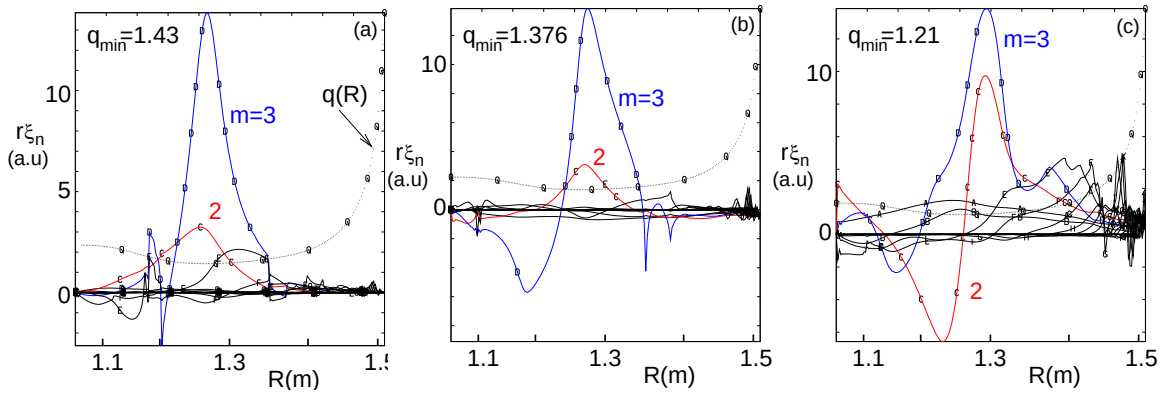

Figure 8: BAAE radial structures as computed by NOVA code for different values of q_{min}, as indicated. Shown in figures is used reversed shear q-profile as was measured by MSE diagnostics.

records the x-ray emission integrated over the chords. Due to strong gradient of the x-ray emission as a first approximation of the mode structure one can take actual signal for the radial structure of BAAE without using sofisticated inversion technique [24]. The evolution of USXR radial mode structure shown in Figures 9(a,b) is remarkably close to the theory predictions. Both the peak of the mode amplitude and its width are apparently similar to BAAE structures shown in Figures 8(a,b). As we noted the BAAE does not seem to enter

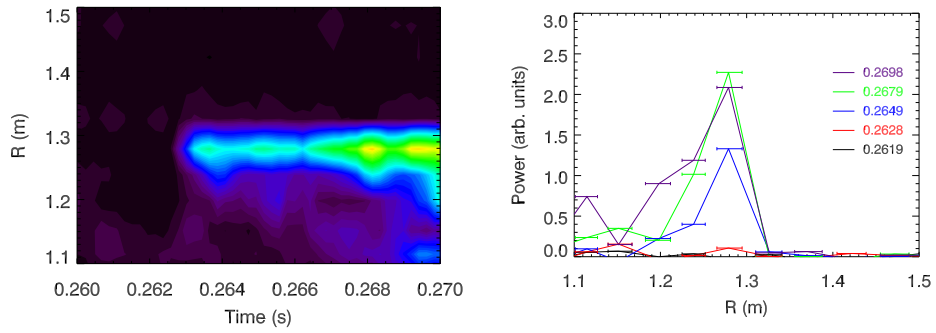

Figure 9: Raw USXR signal temporal behaviour shown as contour map in the plane t, R, figure (a). Shown in figure (b) is the major radius dependence of USXR signal taken at different times over the BAAE frequency sweep, as indicated.

into the BAAE gap completely before possible IRE happened at $t = 0.275s$.

Finally we make a comparison of the BAAE predicted radial displacement structure measured by the microwave reflectometer (local displacement). In each of three discharges three point measurements were taken. These discharges had different plasma densities, which allowed to change the location of the reflectometer points from plasma to plasma. Results and their comparison with NOVA predictions are shown in Figure 10. The vertical axis corresponds to absolute data values for the plasma reported earlier, shot #123816, shown as solid, red circles. Each set of three points of other two plasmas was normalized in such a way that the first point (smallest R value) lays on the theoretical curve. The comparison shows that reflectometer data is in qualitative agreement with NOVA predictions for the BAAE localization. The maximum absolute radial plasma displacement and density perturbation measured by the reflectometer were about $\xi_r/a \sim 10^{-3}$ and $\delta n/n \sim 3 \times 10^{-3}$, respectively.

Note, that because NOVA is ideal MHD code, it can not be relied upon prediction of the localized mode behaviour beyond the point of its interaction with the continuum. In the case of the gap mode, Figure 8(c), it is $R > 1.4m$. At that location the mode conversion is expected from BAAE to Kinetic Alfvén Wave solution (KAW) and at which point high-k measurements were done as presented in Figure 5. Measured range of radial wavevectors is around $k_\perp \simeq 2cm^{-1}$. Longer wavelength channel picks up weaker BAAE signal, which indicates the presence of the conversion layer. Similar observations have been made for the TAE to KAW conversion on TFTR [25].

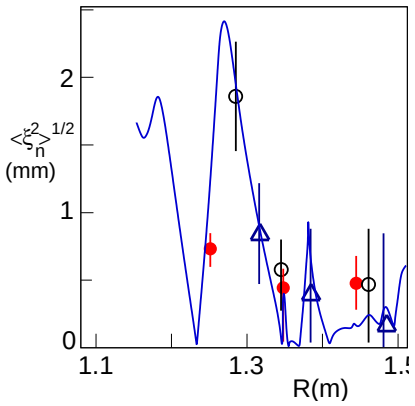

Figure 10: Comparison of NOVA predicted RMS value of normal component of the plasma displacement with the reflectometer measurements for #123816 NSTX shot at $t = 0.27s$ and $n = 2$.

V. SUMMARY AND DISCUSSION

In this paper we presented a theoretical description of the ideal MHD Alfvén - acoustic continuum gap in the limit of low beta and high aspect ratio plasma. Numerically we have found new global eigenmodes, called here BAAEs, which are formed near the extrema points of the continuum in both low and high beta plasmas. We also presented experimental observations, which support qualitatively and quantitatively our theoretical predictions.

In previous work [1] and in this paper we found that ideal MHD simulated BAAE frequency evolution qualitatively agrees with JET observations. Analysis of the monotonic q-profile plasma suggests that at the point when BAAE frequency enters the Alfvén - acoustic its frequency is higher by a factor of 1.77 (1.57 in case of reversed shear profile) than the highest frequency observed for these modes. This is the lowest value ideal MHD can provide by keeping only thermal electron (neglecting bulk ion) pressure. The model for γ as well as kinetic effects such as due to thermal ion FLR and non-perturbative interaction with energetic particles ([19]) may also be responsible for the mismatch in computed and measured mode frequencies.

In this paper we explored another potential ways to reconcile simulations and observations in JET, which is to assume that in the plasma there is a region with local $q_{min} = 1.5$, in which case localized BAAEs with only even toroidal mode numbers can exist ($m = q_{min}n$ must be integer) and the gap BAAE eigenfrequency is 1.5 times lower in simulations. This would

bring NOVA predictions for the BAAE frequency within reasonable uncertainty of 10% to the observed $f = 14kHz$. Therefore, EFIT equilibrium solver prediction that q_0 is close to unity and other observations, such as sawtooth like events soon after BAAE observations, challenges theory. This may be resolved by more detailed measurements of the q-profile. The required current drive profile modification can be due to several effects, such as off-axis ICRH induced current drive, radial transport (and current drive redistribution) of H-minority ions due to MHD activity, such as present TAEs and BAAEs. Finally, in such low density of the plasma a substantial part of the current can be carried by the runaway electrons [**?**].

The study of q-profile by MSE diagnostic was in the center of the recent NSTX experiments reported here where BAAEs were observed. Indeed, even $n = 2, 4$ modes with sweeping frequencies have been observed at the same time when q_{min} was close to 3/2 value. Detailed measurements of the BAAE internal structure revealed the same radial localization, eigenfrequency and their evolution as was predicted by theory. We note, that the reported BAAEs in NSTX seem to stay near the modified Alfvén continuum frequency and do not enter the Alfvén - acoustic gap. BAAEs are typical for NSTX high beta plasma and strong beam ion population. A strong drive is required in NSTX where electron and ion temperatures are similar so that strong ion Landau damping is also expected, which is likely due to acoustic mode coupling. However, if both the drive and the damping are strong one can expect that BAAEs open a potential energy channeling from beam ions directly to thermal ions without goind first to the electrons. This is similar to the idea of α-channeling suggested for tokamaks [26].

As we mentioned, Alfvén - acoustic continuum was studied in previous publications with the expressions for GAM (or BAE) branches obtained in [4, 12–15]. Kinetic theory of Ref. [15] does not seem to include acoustic sideband harmonic coupling, so that BAAE gap frequencies were not reported. Expression for the Alfvén - acoustic continuum at the rational surface was found in Ref. [6], whereas numerically BAAE gap structure is shown in Ref. [7]. Global modes corresponding to GAM frequency and called BAE were found in Ref. [27] and in Ref. [7]. It is clear that the antenna version of the code of Ref. [7] picked up the global mode, which had a strong interaction with the continuum and the eigenfrequency, which is close to the GAM (BAE). More localized global BAAEs with the frequencies below the GAM frequency were not seen in the plasma response. BAAE gap frequency ratio to GAM frequency is $1/\sqrt{2\left(q^2+1\right)}$, but both scale the same way with

regard to the plasma parameters. However, the frequency evolution of BAAE (especially the one at the low shear or core region) is notably different from that expected for the GAM (BAE) frequency. Finally, the GAM (BAE) frequency is substantially higher than the BAAE frequency obtained in our work.

Our BAAE based interpretation of JET and NSTX observations is apparently different from the interpretation of low frequency activity in DIII-D [28], which are based on BAE simulations described in Ref.[27]. In that reference BAEs, which matched the measured frequencies, were obtained numerically by neglecting the acoustic wave coupling. This procedure did not provide any reasonable and physical mode structures in NOVA simulations of both JET and NSTX plasmas considered due to the strong interaction with the continuum.

The use of BAAE measurements, as we have shown in the example of a JET plasma simulations, can potentially extend the MHD spectroscopy to determine q_0, especially in high-β plasmas. Such observations could be a very important diagnostic tool for ITER and other burning plasma experiments. These observations would also help to infer the central plasma beta and the ion and electron temperatures by reconciling the measurements and the theory.

---

[1] N. N. Gorelenkov, H. L. Berk, E. Fredrickson, and S. E. Sharapov, Phys. Letters A p. doi:10.1016/j.physleta.2007.05.113 (2007).

[2] N. N. Gorelenkov, H. L. Berk, and E. D. Fredrickson, Bull. Amer. Phys. Society (abstract NO1 10) **51**, 183 (2006).

[3] J. P. Goedbloed, Phys. Fluids **18**, 1258 (1975).

[4] M. S. Chu, J. M. Greene, L. L. Lao, A. D. Turnbull, and M. S. Chance, Phys. Fluids B **11**, 3713 (1992).

[5] J. P. Goedbloed, Phys. Plasmas **5**, 3143 (1998).

[6] B. van der Holst, A. J. C. Beliën, and J. P. Goedbloed, Phys. Plasmas **7**, 4208 (2000).

[7] G. T. A. Huysmans, W. Kerner, D. Borba, H. A. Holties, and J. P. Goedbloed, Phys. Plasmas **2**, 1605 (1995).

[8] C. Z. Cheng and M. S. Chance, Phys. Fluids **29**, 3695 (1986).

[9] C. Z. Cheng, Phys. Reports **211**, 1 (1992).

[10] N. Gorelenkov, G. Kramer, and R. Nazikian, Plasma Phys. Control. Fusion **48**, 1255 (2006).

[11] A. B. Mikhailovskii and S. E. Sharapov, Plasma Phys. Rep. **25**, 838 (1999).

[12] N. Winsor, J. L. Johnson, and J. M. Dawson, Phys. Fluids **11**, 2448 (1968).

[13] B. N. Breizman, S. E. Sharapov, and M. S. Pekker, Phys. Plasmas **12**, 112506 (2005).

[14] H. L. Berk, C. J. Boswell, D. N. Borba, A. C. A. Figueiredo, T. Johnson, M. F. F. Nave, S. D. Pinches, and S. E. Sharapov, Nucl. Fusion **46**, S888 (2006).

[15] F. Zonca, L. Chen, and R. Santoro, Plasma Phys. Contr. Fusion. **38**, 2011 (1996).

[16] B. N. Breizman, H. L. Berk, M. S. Pekker, S. D. Pinches, and S. E. Sharapov, Phys. Plasmas **10**, 3649 (2003).

[17] S. E. Sharapov, A. B. Mikhailovskii, and G. T. A. Huysmans, Phys. Plasmas **11**, 2286 (2004).

[18] G. Y. Fu and H. L. Berk, Phys. Plasmas **13**, 052502 (2006).

[19] N. N. Gorelenkov and W. W. Heidbrink, Nucl. Fusion **42**, 150 (2002).

[20] V. A. Mazur and A. B. Mikhailovskii, Nucl. Fusion **17**, 193 (1977).

[21] G. J. Kramer, N. N. Gorelenkov, R. Nazikian, and C. Z. Cheng, Plasma Phys. Contr. Fusion **46**, L23 (2004).

[22] E. D. Fredrickson, N. A. Crocker, N. N. Gorelenkov, W. W. Heidbrink, S. Kubota, F. M. Levinton, H. Yuh, J. E. Menard, and R. E. Bell, Phys. Plasmas **14**, submitted (2007).

[23] M. A. V. Zeeland, G. J. Kramer, M. E. Austin, R. L. Boivin, W. W. Heidbrin, M. A. Makowski, G. R. McKee, R. Nazikian, W. M. Solomon, and G. Wang, Phys. Rev. Letters **97**, 135001 (2006).

[24] E. D. Fredrickson, R. E. Bell, D. Darrow, G. Fu, N. N. Gorelenkov, B. P. LeBlanc, S. S. Medley, J. E. Menard, H. Park, A. L. Roquemore, et al., Phys. Plasmas **13**, 056109 (2006).

[25] K. L. Wong, N. Bretz, G. Y. Fu, J. Machuzak, J. R. Wilson, Z. Chang, L. Chen, D. K. Owens, and G. Schilling, Phys. Letters A **224**, 99 (1996).

[26] N. J. Fisch and J.-M. Rax, Phys. Rev. Lett. **69**, 612 (1992).

[27] A. D. Turnbull, E. J. Strait, W. W. Heidbrink, M. S. Chu, H. H. Duong, J. M. Greene, L. L. Lao, T. S. Taylor, and S. J. Thompson, Phys. Fluids B **5**, 2546 (1993).

[28] W. W. Heidbrink, E. J. Strait, M. S. Chu, and A. D. Turnbull, Phys. Rev. Letter **71**, 855 (1993).